International Journal of Scientific Engineering and Science
Volume 8, Issue 5, pp. 64-69, 2024. ISSN (Online): 2456-7361

Establishment of Material Removal Rate Model for Magnetorheological Polishing of Optical Lens Surface Using a Circular Magnet Array

Nguyen Duc Minh[1], Nguyen Ngoc Quan[1,*], Hoang Van Thang[1], Nguyen Van Hoang[1], Quach Vu Hieu[1]

[1]School of Mechanical and Automotive Engineering, Hanoi University of Industry, 298 Cau Dien, Bac Tu Liem District, Ha Noi, Vietnam

Abstract— *In various fields such as aerospace, healthcare, optics, etc., there is an increasing demand for higher precision, necessitating enhanced accuracy down to the smallest details. Surface micro-roughness is one of the critical aspects, and to improve quality, the mathematical model of the material removal process in magnetorheological polishing has been widely applied. A mathematical model has been created to calculate the properties of polishing based on the technique of surface improvement using magnetorheological finishing (MRF). This article presents a methodology for predicting the shape and size of a function that affects the quality of the surface. The next section discusses the impact of this function on material removal rates. This new model inherits and contributes to improving both accuracy and cost-effectiveness. Additionally, it allows polishing even more complex surfaces, marking the first step in providing influencing function timelines*.

Keywords— *Magnetorheological Finishing, Material removal rate, Abrasive grain, Surface Finishing, Circular magnet array*.

I. INTRODUCTION

Magnetorheological finishing (MRF) methods have become a significant trend in the field of precision optics, where there is a high demand for the accuracy of aspherical components. Special-shaped polished surfaces cannot be processed using conventional methods [1-3], so new methods such as magnetorheological polishing (MRP) have been developed to meet this demand. MRP workpieces a small contact area polishing tool to locally remove material. The MRP process is pre-computed based on surface error profiles and material removal characteristics of the tool [4]. Time dwell techniques are applied to control the amount of material removed, with direct influence based on the tool's movement speed. In modern manufacturing, MRP offers high predictability and precision, making it an essential tool for producing cost-effective and high-quality surfaces [5, 6]. However, challenges still exist in the use of MRP processes. The influencing function, a crucial factor in the process, often requires diverse materials and lengthy trial-and-error evaluations, impacting both time and cost [7]. Additionally, difficulties may arise when dealing with aspherical or freeform surfaces in time dwell methods. To address these limitations, a new mathematical approach based on the influencing function model has emerged. This method eliminates complex measurements and the need for additional workpiece samples, resulting in improved cost-effectiveness and economic efficiency [8-10]. The influencing function model significantly aids in solving tool tracking problems, ensuring high accuracy, and providing flexibility.

The surface finishing technique using MRF with abrasive particles is the basis for establishing a new influencing function contributing to the processing of challenging surfaces [11-14]. This paper addresses the contact region between the machined surface of the workpiece and the machine tool, subsequently calculating the impact of the influencing function on material removal.

II. MAGNETORHEOLOGICAL FLUID SURFACE FINISHING TECHNIQUE USES A CIRCULATING MAGNETIC ABRASIVE PARTICLE FLOW

The basic concept of MRF is the use of magnetorheological fluid with abrasive properties as a tool for polishing [15-17]. A pump facilitates the delivery of the fluid to a spraying device, which is then utilized to spray the fluid onto the grinding wheel. Magnets installed inside the wheel generate a magnetic field, attracting the abrasive particles. When subjected to the force from the magnetic field, the abrasive particles must follow the grinding motion of the wheel. The fluid becomes a tool for subaperture polishing (see Fig. 1). A suction port draws the fluid from the grinding mechanism, and then the regulated fluid is returned to the working area, forming a closed-loop process. The formation of a closed-loop circulation process aims to maintain the fluid within the grinding wheel chamber, ensuring the tool remains in a consistent state.

CNC-operated positioning components control the process through a magnetically solidified liquid on the grinding wheel, utilizing a 3-axis control system. Since axis A rotates simultaneously, the entire working surface can be cleaned. The amount of material removed from each point on the work surface is based on the contact time of each point with the liquid in the polishing region. For each point, an increased contact time leads to a greater amount of material being cut, and vice versa. Exposure time is estimated using residence time calculation profiles.

2.1. MRF and its impact on the influencing function

The influencing function is crucial for describing the material removal characteristics of the polishing tool. The

International Journal of Scientific Engineering and Science
Volume 8, Issue 5, pp. 64-69, 2024. ISSN (Online): 2456-7361

influencing function has two important components: geometric size and material removal distribution. In the first part of the study, we attempted to predict the magnitude and shape of the influencing function. The second part of the study will discuss the method for calculating material removal characteristics within the influencing function.

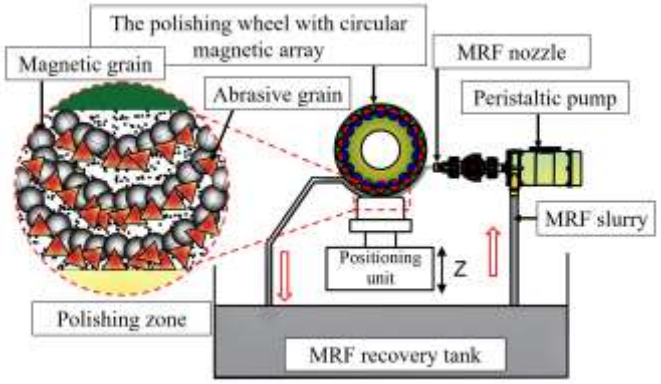

Fig. 1. Diagram of MRF process

Typically, data arrays represent various functions, and the size of the influencing function in the context refers to the corresponding physical dimensions of the polishing machine. These dimensions are calculated based on the utilization of the ratios of the cells within the data array.

2.2. Tool utilization in the MRF polishing process

The continuous flow of abrasive liquid is crucial in the MRF process. When a magnetic field is present, the liquid is drawn into the grinding wheel, resulting in obtaining the circumferential velocity of the wheel. The form of the liquid is influenced by the wheel's rotation speed, the strength of the magnetic field, and the liquid volume, all of which are modified by the pump's velocity.

Description of the surface error configuration of a typical lens, measured using the interferometric method. Different shades of gray represent the degree of deviation of the optical surface from a perfect sphere, expressed in micrometers (μm). The lens polishing tool (fluid) interacts with The lens polishing tool (liquid) interacts with the lens for a certain period of time (Fig. 2). Thus, differences from the processed positions can be observed. The influencing function is calculated after observation, measurement, and recalculation.

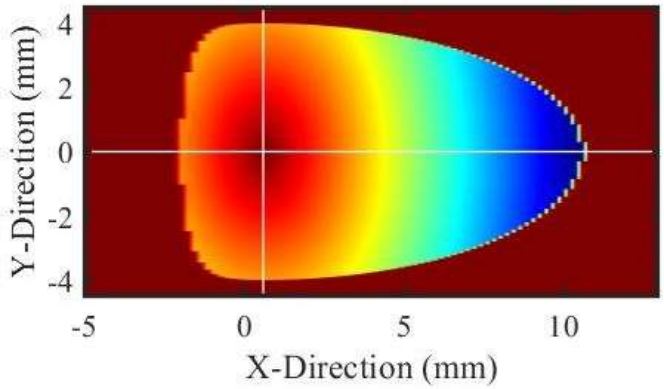

Fig. 2. Influence function obtained as a result.

With experiments demonstrating that an increase in the grinding wheel speed leads to a higher removal volume of liquid per unit time, affecting both the depth and width of the solution. Through observations, it has been noted that enhancing the magnetic field intensity also influences the liquid volume, reducing its width. Similarly, increasing the pump speed helps increase the liquid volume on the grinding surface in both width and height (Fig. 3).

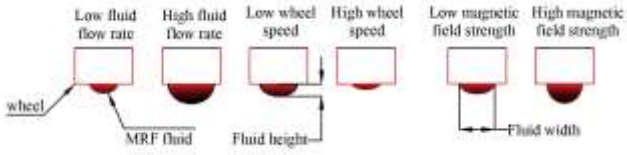

Fig. 3. Different shapes of liquids on polishing wheel

2.3. Mathematical formulation of the polishing tool

The polishing process using this magnetically driven circulating method involves creating and controlling the polishing compound based on rheological properties, primarily the external energy cluster, such as the magnetic field. The magnetorheological fluid, under the control of the magnetic field, can dynamically adjust its viscosity between liquid and solid states. Moreover, it enables swift balance adjustments within milliseconds, contributing to improved polishing by autonomously regulating pressure. However, in the absence of a magnetic field, the particle flow exhibits properties similar to a Newtonian fluid. Furthermore, when a magnetic field is present, the particles operate on the principles of Bingham plasticity, described mathematically as follows.

$$\tau = \eta\dot{\gamma} + \tau_0(H) \text{ for } \tau_0 \le \tau, \quad (1)$$

$$\tau = 0 \text{ for } \tau_0 > \tau,$$

Here, represents the dynamic viscosity, influenced by the composition of the base fluid, is the applied stress, and is the stress induced by the field, dependent on the strength of the magnetic field (H), represents the rate of shear.

The magnetically driven abrasive fluid is formulated using a solution containing magnetic iron carbonyl particles, a cooling fluid, and non-magnetic abrasive particles. Iron carbonyl play a crucial role in stiffening the fluid under the influence of a magnetic field [18, 19]. For surface interaction, abrasive particles like cerium oxide or diamond are commonly employed. This fluid plays a vital role in rheological properties, primarily composed of water and stabilizing agents. The presence of water and stabilizing agents is essential to prevent the oxidation of iron particles and inhibit agglomeration [20, 21]. The base abrasive fluid, a key component in the experiments described in the article, consists of approximately 3% stabilizing agent, around 6% cerium oxide, followed by 35% iron carbonyl particles, and the majority is water. The magnetic field effect generates a chain-like structure around the abrasive iron carbonyl particles during the grinding process. The polishing compound [22] is a combination of iron carbonyl particles, abrasive particles, along with a fluid influenced by magnetic forces.

Observations during the magnetorheological finishing process indicate that in the polishing zone, the flow of

International Journal of Scientific Engineering and Science
Volume 8, Issue 5, pp. 64-69, 2024. ISSN (Online): 2456-7361

abrasive particles takes on a pyramid-like shape. The shape of the magnetorheological fluid resembles a parabola and is mathematically described as follows:

$$y = a_1x^2 + b_1x + c_1 \quad (2)$$

Information about the liquid flow rate is continuously updated based on static pressure measurements and flow measurements in the spray nozzle, providing insights into the viscosity of the liquid during the surface finishing process. The grinding wheel has the ability to adjust its rotational speed through a servo motor. The following is the foundational calculation to determine the cutting area of the liquid, as depicted in Figure 3, and is expressed as follows:

$$A = \frac{1}{v}.\dot{V} \quad (3)$$

In which: represents the flow rate of the fluid, and 'v' denotes the peripheral velocity of the grinding, determined by:

$$v = 2\pi.r.f \quad (4)$$

In particular, r is the radius of the bread and f is the rotation speed of the grinding.

The width and height dimensions of the liquid (seen in Figure 3) can be optically measured with a resolution of 0.01 mm. However, measurements in both dimensions can be easily taken using calipers and sensors.

Figure 1 depicts the integrated sensor head in the positioning unit. Adjusting the z-axis until the sensor head makes contact with the liquid provides information about the height of the liquid. The accuracy of both measurement methods is approximately 0.1 mm. To avoid magnetic interference during measurements, it should be noted that both the caliper and the sensor head are constructed from non-magnetic materials.

Four parameters are known to describe a pyramid shape. However, if Equation (2) is used to define the pyramid shape, it may lead to over-determination. Equation (5) is chosen to describe a pyramid with four parameters while ensuring the symmetry of the pyramid along the axis, with the additional element being :

$$y = a_2x^4 + b_2x^2 + c_2x + d \quad (5)$$

The coefficients a, b, c, and d are computed through the following system of equations:

$$\begin{aligned} z_1 &= y_1^4 a. + y_1 c. + y_1^2 b. + d, \\ z_2 &= y_2^4 a. + y_2 c. + y_2^2 b. + d, \\ z_3 &= y_3^4 a. + y_3 c. + y_3^2 b. + d, \\ A &= \left[(y_3^5 - y_1^5).\frac{a}{5} \right] + \left[\left(y_3^3 - y_1^3 \right).\frac{c}{2} \right] + \left[\left(y_3^3 - y_1^3 \right).\frac{b}{3} \right] + (y_3 - y_1).d, \end{aligned} \quad (6)$$

Where:

$$\begin{aligned} & y_1 = -\frac{1}{2}.f_{width}; z_1 = 0; y_2 = 0 \\ & z_2 = f_{height} + offset; z_3 = 0; y_3 = \frac{1}{2}.f_{width} \\ & A = f_{area} + whell_{area} \end{aligned} \quad (7)$$

The compensation is calculated as follows:

$$\begin{aligned} offset &= r.2.\left(\sin\left(\varphi.\frac{1}{4} \right) \right)^2, \\ \varphi &= 2.\arcsin\left(f_w.\frac{1}{2.r} \right), \end{aligned} \quad (8)$$

Where r represents the radius of the polishing wheel. It's important to note that the parabola's area is the summation of the area determined by the speed of the liquid line, the liquid area, and the area of the grinding, the bread area (refer to Fig. 4).

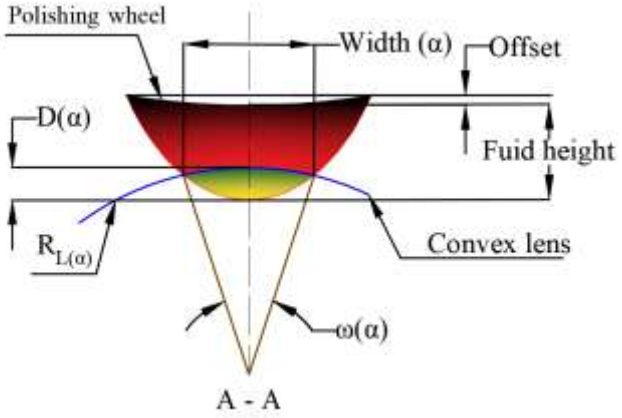

Fig. 4. The MRF shape in polishing process

$$wheel_{area} = \frac{1}{2}\left(\varphi - \sin(\varphi) \right).r^2, \quad (9)$$

Here, 'r' represents the radius of the grinding wheel, and θ is the angle calculated according to formula (7), a = 0.0376, b = ÿ×0.3921, c = 0, and d = 0.9842.

III. PREDICTING THE STRUCTURE OF AN IMPRESSION FUNCTION

By calculating the intersection of the working surface with the grinding machine, predictions can be made regarding the visual appearance and dimensions of the influencing function. However, for each actual shape that the grinder encounters, parameters need to be adjusted to obtain the appropriate intersection point. Therefore, flat shapes, have been provided with mathematical models to differentiate between these specific forms.

3.1. Machining of a convex surface

In Fig. 5, the geometric relationship between a concave work surface and the liquid on the grinding wheel is depicted. The maximum angle can be calculated using parameters such as the workpiece's immersion depth in the liquid and the height of the liquid.

$$\begin{aligned} R_P &= -D + R_L + R_F, \\ R_F &= H_F + R_W, \\ \alpha_{\max} &= \arccos\left(-(R_F^2 - R_L^2 - R_P^2).\frac{1}{2.R_L.R_P} \right), \end{aligned} \quad (10)$$

International Journal of Scientific Engineering and Science
Volume 8, Issue 5, pp. 64-69, 2024. ISSN (Online): 2456-7361

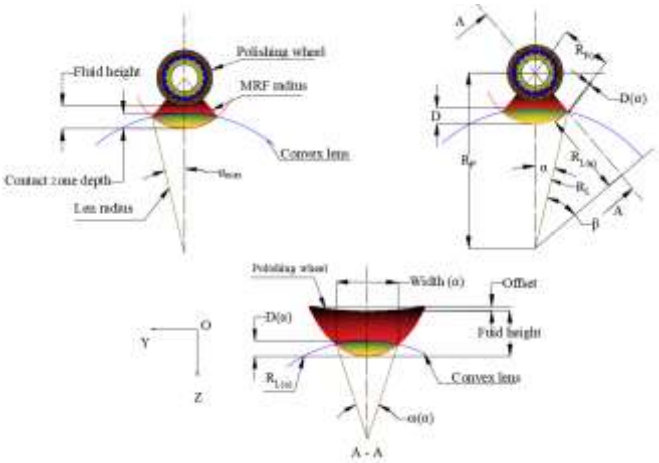

Fig. 5. Geometric relationship for convex processing surface

Where is the radius of the grinding wheel, is the height of the liquid, is the radius of the workpiece, and D is the immersion depth of the workpiece in the liquid. is the radius of the liquid, and is the radius of the rotating axis, both are intermediate results to simplify the equation for α max.

In this context, R_W is the radius of the grinding wheel, R_L is the radius of the workpiece, and *D* is the immersion depth of the workpiece. H_F represents the height within the liquid. R_F is the radius of the liquid, and R_P is the radius of the rotating axis. Both R_P and R_F serve as intermediate results to simplify the equation for the α maximum.

The radius of the liquid R_F can be calculated as a function of the α:

$$R_F(\alpha) = \sqrt{R_L^2 - 2.R_L.R_P.\cos(\alpha) + R_P^2} \tag{11}$$

Equation (10) allow the calculation of corner *B*, in turn bring δ angle:

$$\beta = \arccos\left(-(R_L^2 - R_F^2(\alpha) - R_P^2)\frac{1}{2.R_F(\alpha).R_P}\right), \qquad \delta = \frac{\pi}{2} - \beta - \alpha \tag{12}$$

Calculation of special embryo radius $R_L(\alpha)$, this becomes significant in subsequent steps; for now, it is feasible:

$$R_L(\alpha) = \sin(\delta).R_L \tag{13}$$

The depth of the embryo in the liquid also changes, and is a function of α angle:

$$D(\alpha) = -R_{F(\alpha)} + R_F \tag{14}$$

The shape of the parabola is determined by the mathematical model of the polishing tool. The depth of the embryo soaked in liquid and embryo radius, such as the jaws of the corner, have been described above and therefore also known.

Hence, we can establish the following set of equations:

$$z_s = y^4 a + yc + y^2 b + d$$
$$z_s = \left(R_L(\alpha) - \sqrt{R_L^2(\alpha) - y^2}\right) + H_F - D(\alpha) + offset \tag{15}$$

For every α angle between the workpiece and the pyramid shape ranging from 0 to its maximum value, there are two intersection points. An example is the y coordinate, which can be calculated using approximate mathematical methods. The distance between these intersection points then determines the width of the influence function based on the α angle. Fig. 6 visually illustrates an example result that is very similar to the actual shape of the influence function (see Fig. 2). However, this computational form of the influence function is a design representation. To determine the actual shape, the arc length of a given α angle (section A-A in Figure 5) requires knowledge of angle ω:

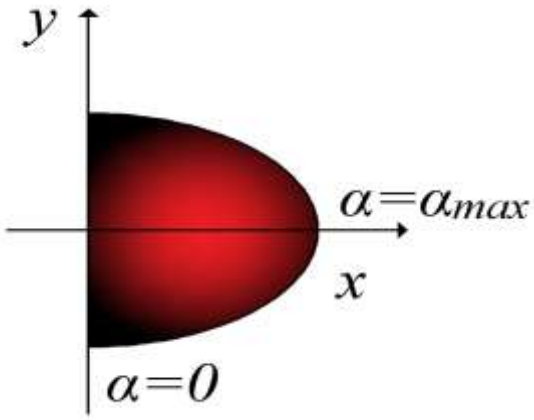

Fig. 6. Calculation form of α angular indentation function (from 0 to maximum) (from 0 to the maximum)

$$\omega(\alpha) = 2.\arcsin\left(\frac{1}{2.R_L(\alpha)}.width(\alpha)\right), \qquad width_{true}(\alpha) = \omega(\alpha).R_L(\alpha) \tag{16}$$

Experimental results, presented by the following, shows that the actual width of a function is greater than that of the actual width that has been converted, defined by the equation (16). Therefore, a k_{width} factor is integrated to approximate the actual shape of an influence function:

$$width_{real}(\alpha) = k_{width}.width_{true}(\alpha) \tag{17}$$

3.3. Optimizing Influence Function Structure

The influence function is elliptical in shape, a result of extensive calculations involving the intersection between the surface of the part and the fluid on the wheel. However, this elliptical representation is not complete; it can be considered as an approximate value obtained by compressing it along the major axis (Figure 2). A more effective approach to refine and approximate the shape based on real experimental data of the influence function involves compressing it along the x-axis while simultaneously calculating the changes in αvalues, ranging from the smallest to the largest (as depicted in Figure 6) along the y-axis. Figure 8 illustrates the results, demonstrating similarity to the shape shown in Figure 2.

In examining the compression level of the influence function's shape, we compute the compression coefficient

International Journal of Scientific Engineering and Science
Volume 8, Issue 5, pp. 64-69, 2024. ISSN (Online): 2456-7361

k_{ratio}. This coefficient hinges on the surface shape of the workpiece, reflecting the actual length ratio of the influence function below and above the grinding wheel. For convex and concave workpiece surfaces, the compression ratio of the influence functions is ascertained using the following formula:

$$k_{ratio} = \frac{\varphi_1}{\varphi_2 + \varphi_1} \quad (18)$$

The typical value for k_{ratio} is approximately 0.8. To approximate the width, an additional factor$k_{width}$is introduced. Observations indicate that the actual length exceeds the ideal mathematical length in practical experiments. Therefore, permitting the elongation of the influence function shape in the x-direction by k_{length}. The associated factor for the length k_{length}characterizes the ratio between $\varphi_1$and $\alpha_{max}$for the local convex and concave surface influence functions of the workpiece requiring processing:

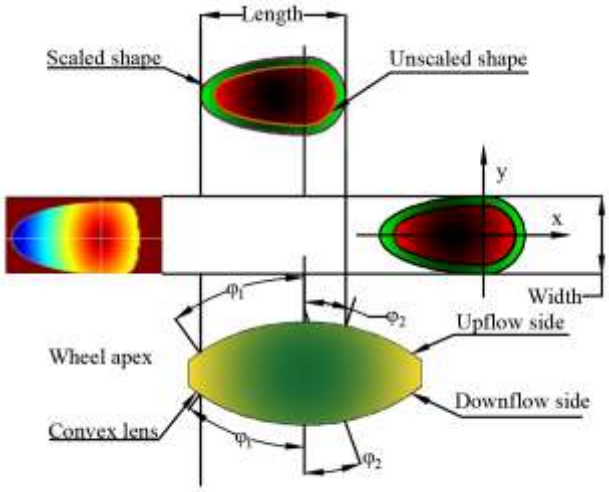

Fig. 8. The calculated scaling of the influencing function's shape

$$k_{length} = \frac{1}{\alpha_{\max}} . \varphi_1 \quad (19)$$

Fig. 8 demonstrates the mathematically optimized transformation that is performed as a function of influence in compression and reflection, as described above. The passive mode is similar to the active mode, but is larger in scope. Therefore, the ratio structure is created by extending the positive mathematical equation along the x and y directions using the local and general coefficients $k_{width}$and k_{length}.

III. DISCUSSION

In Fig. 8, the computed cross-section of the influencing function closely resembles the actual shape determined in practice. The deformable nature of the liquid, acting as a polishing tool, leads to its flattening upon contact with the workpiece surface. Since the liquid remains in a dispersed state, the majority of material removal occurs through the upper part of the wheel. Consequently, the shape of the influencing function for a Magnetorheological Finishing (MRF) is akin to that of a conventional iron, rather than a complete ellipse as would be the case in an ideal intersection. Consequently, additional parameters, including coefficients k_{length} and k_{width}, must be introduced into the calculations to accurately describe the actual shape of the function's influence. The final demonstrates that a coefficient of 1.1 is sufficient to predict and reproduce the actual length accurately. To approximate the actual width, calculating the magnitude of the influence function's width necessitates a coefficient of approximately 1.8.

Experimental results show a similar paraboloid shape, and the dimensions of the influence function are quite similar, varying only with changes in wheel speed, pump speed, and magnetism. The outcome is paraboloids with similar shapes, raised or lowered (depending on the volume of liquid on the wheel) according to the direction of movement. The radius of the machined part was the only variable. The liquid on the grinding wheel takes on a narrow strip formation, so the length of the influence function increases much faster than the width, especially for convex curved surfaces. This indicates that the radius of the machined part significantly affects the length of the influence function but does not have much impact on its width. The developed model of the influence function goes beyond the current complex process to accurately determine the influence function, overcoming the challenges of traditional testing methods. As a result, the manufacturing process has been significantly improved, becoming more cost-effective. Compared to the current method, the model does not require any additional samples of the machined part. Moreover, there is no material contact with the surface through the polishing tool. The absence of physical uncertainty and the absence of a sample part mean no pre-measurements and post-measurements, eliminating measurement errors entirely and reducing inaccuracies in the determination process. Therefore, there is no requirement to verify the quality of the influence function since the function is calculated symmetrically.

The polishing process to achieve high-quality results often requires an accurate influence function. To adjust and determine a well-adjusted influence function, the intervention of trained and experienced technical personnel is often required. This involves considerable experimentation time and material. On the other hand, a mathematical model can serve as a substitute to increase the accuracy of the influence function for specific parameters or a specific target that can be computed efficiently without forming additional components, thereby improving the disadvantages associated with traditional methods used for a long time.

If the obtained processing time significantly exceeds the minimum processing time, the dimensions of the influencing function may not be suitable for the process. Adjusting the parameters enables fine-tuning of the influencing function and minimizes processing time. However, gathering information about the new influencing function requires a defined process. Once again, the mathematical model of the influencing function proves highly useful for quickly optimizing the influencing function. The first part of the model calculates the

shape of the influencing function for convex, concave, and flat surfaces. For a complex free-form surface, it can be approximated locally by surface material. This model allows predicting the influencing function for each position of the polishing tool on the surface. Any changes in the influencing function during the polishing process can be taken into account before calculating the storage time, thus aiding in achieving a high-quality surface.

Not only the preservation time method but also the well-defined variation of the influencing function during the polishing process can be used to control material removal effectively [28]. However, this method requires accurate knowledge of the relationship between the tool parameters, the machined part, and the obtained influencing function. The mathematical model provides these relationships and is the first step towards this novel approach.

V. Conclusion

The development of a predictive model for the function of removing the material marks a significant advancement. The initial section outlines the computation of the influence function's shape and size. Derived from practical experiments to validate the model, several key observations have been made: Utilizing straightforward geometric relationships for calculating the influence function size and shape yields highly accurate predictions across diverse MRF parameter configurations. The method of using the influence function to determine sizes and shape calculations holds promising developments for the future, given its highly accurate predictions across various MRF parameter settings. Consequently, there is no need for complex fluid mechanics models as the computer can accurately predict their shapes. Surface material can be adjusted based on the influence function, enhancing the quality of the final surface through time-dependent storage methods. Furthermore, this advanced approach has the potential to expedite the implementation process and serves as a foundational model that can further develop the application of time-variable influence functions.

To sum up, the developed influence function model streamlines the swift computation of polishing tool characteristics, playing a pivotal role in advancing computer-controlled polishing processes. This advancement positively impacts both economic and product quality aspects in precision surface manufacturing. Consequently, this innovative approach isn't limited to MRF alone; other polishing methods relying on error and necessitating influence functions for polishing process calculations can also reap the benefits of this novel methodology.

References

1. Ghosh, G., A. Sidpara, and P.P. Bandyopadhyay, Review of several precision finishing processes for optics manufacturing. 2018. 1: p. 170-188.
2. Xie, M., et al., Review on Surface Polishing Methods of Optical Parts. Advances in Materials Science and Engineering, 2022. 2022: p. 8723269.
3. Li, W., et al., A Review of Emerging Technologies in Ultra-Smooth Surface Processing for Optical Components. Micromachines, 2024. 15(2).
4. Guo, Z., et al., Analysis on a deformed removal profile in FJP under high removal rates to achieve deterministic form figuring. Precision Engineering, 2018. 51: p. 160-168.
5. Schinhaerl, M., et al., Mathematical modelling of influence functions in computer-controlled polishing: Part II. Applied Mathematical Modelling - APPL MATH MODEL, 2008. 32: p. 2907-2924.
6. Wan, S., et al., Modeling and analysis of sub-aperture tool influence functions for polishing curved surfaces. Precision Engineering, 2017. 51.
7. Abubakar, A.M., et al., Knowledge management, decision-making style and organizational performance. Journal of Innovation & Knowledge, 2019. 4(2): p. 104-114.
8. Zha, J., et al., An accuracy evolution method applied to five-axis machining of curved surfaces. The International Journal of Advanced Manufacturing Technology, 2023. 125(7-8): p. 3475-3487.
9. Mohamed, A., et al., Tool Condition Monitoring for High-Performance Machining Systems-A Review. Sensors (Basel), 2022. 22(6).
10. Xie, M., et al., Review on Surface Polishing Methods of Optical Parts. Advances in Materials Science and Engineering, 2022. 2022.
11. Schinhaerl, M., et al., Mathematical modelling of influence functions in computer-controlled polishing: Part II. Applied Mathematical Modelling, 2008. 32(12): p. 2907-2924.
12. Schinhaerl, M., et al., Calculation of MRF influence functions - art. no. 66710Y. 2007. 6671.
13. Bai, Y., et al., Material removal model of magnetorheological finishing based on dense granular flow theory. Light: Advanced Manufacturing, 2022. 3(4).
14. Yang, B., et al., Material removal model of magnetorheological finishing based on dense granular flow theory. Light: Advanced Manufacturing, 2022. 3(4): p. 630-639.
15. Shimada, K., Y. Wu, and Y. Wong, Effect of magnetic cluster and magnetic field on polishing using magnetic compound fluid (MCF). Journal of Magnetism and Magnetic Materials - J MAGN MAGN MATER, 2003. 262: p. 242-247.
16. Zheng, Y., The Most Suitable Clearance in MCF (Magnetic Compound Fluid) Polishing. Journal of Advance Research in Mechanical & Civil Engineering (ISSN: 2208-2379), 2016. 3: p. 13-18.
17. Li, X., et al., Investigation on Polishing the Concave Surface of Zirconia Ceramics with Magnetic Compound Fluid Enhanced by Hydration Reaction. Magnetochemistry, 2023. 9(3).
18. Kwon, S., et al., Magnetorheology of xanthan-gum-coated soft magnetic carbonyl iron microspheres and their polishing characteristics. Journal of the Korean Physical Society, 2013. 62.
19. Yu, M., et al., Influence of composition of carbonyl iron particles on dynamic mechanical properties of magnetorheological elastomers. Journal of Magnetism and Magnetic Materials, 2012. 324(13): p. 2147-2152.
20. Davoodi, S., et al., Synthetic polymers: A review of applications in drilling fluids. Petroleum Science, 2023.
21. Zhu, W.-L. and A. Beaucamp, Compliant grinding and polishing: A review. International Journal of Machine Tools and Manufacture, 2020. 158: p. 103634.
22. Salem, A.M.H., et al., Effect of Carbonyl Iron Particle Types on the Structure and Performance of Magnetorheological Elastomers: A Frequency and Strain Dependent Study. Polymers (Basel), 2022. 14(19).